

# Evidence against aquaporin-1-dependent CO<sub>2</sub> permeability in lung and kidney

Xiaohui Fang, Baoxue Yang, Michael A. Matthay and A. S. Verkman

Departments of Medicine and Physiology, Cardiovascular Research Institute, University of California, San Francisco, CA 94143-0521, USA

AQP1-dependent CO<sub>2</sub> transport has been suggested from the increased CO<sub>2</sub> permeability in *Xenopus* oocytes expressing AQP1. Potential implications of this finding include AQP1-facilitated CO<sub>2</sub> exchange in mammalian lung and HCO<sub>3</sub><sup>-</sup>/CO<sub>2</sub> transport in kidney proximal tubule. We reported previously that: (a) CO<sub>2</sub> permeability in erythrocytes was not affected by AQP1 deletion, (b) CO<sub>2</sub> permeability in liposomes was not affected by AQP1 reconstitution despite a 100-fold increased water permeability, and (c) CO<sub>2</sub> blow-off by the lung in living mice was not impaired by AQP1 deletion. We extend these observations by direct measurement of CO<sub>2</sub> permeabilities in lung and kidney. CO<sub>2</sub> transport across the air-space–capillary barrier in isolated perfused lungs was measured from changes in air-space fluid pH in response to addition/removal of HCO<sub>3</sub><sup>-</sup>/CO<sub>2</sub> from the pulmonary artery perfusate. The pH was measured by pleural surface fluorescence of a pH indicator (BCECF–dextran) in the air-space fluid. Air-space fluid pH equilibrated rapidly ( $t_{1/2} \approx 6$  s) in response to addition/removal of HCO<sub>3</sub><sup>-</sup>/CO<sub>2</sub>. However, the kinetics of pH change was not different in lungs of mice lacking AQP1, AQP5 or AQP1/AQP5 together, despite an up to 30-fold reduction in water permeability. CO<sub>2</sub> transport across BCECF-loaded apical membrane vesicles from kidney proximal tubule was measured from the kinetics of intravesicular acidification in response to rapid mixing with a HCO<sub>3</sub><sup>-</sup>/CO<sub>2</sub> solution. Vesicles rapidly acidified ( $t_{1/2} \approx 10$  ms) in response to HCO<sub>3</sub><sup>-</sup>/CO<sub>2</sub> addition. However the acidification rate was not different in kidney vesicles from AQP1-null mice despite a 20-fold reduction in water permeability. The results provide direct evidence against physiologically significant transport of CO<sub>2</sub> by AQP1 in mammalian lung and kidney.

(Received 14 November 2001; accepted after revision 8 December 2001)

**Corresponding author** A. S. Verkman: Cardiovascular Research Institute, 1246 Health Sciences East Tower, Box 0521, University of California, San Francisco, San Francisco, CA. 94143-0521, USA. Email: verkman@itsa.ucsf.edu

Facilitated transport of CO<sub>2</sub> by aquaporin-1 (AQP1) water channels has been suggested from comparative measurements on control and AQP1-expressing *Xenopus* oocytes. Nakhoul *et al.* (1998) reported a 30–40% increased rate of cytoplasmic acidification after CO<sub>2</sub> exposure in AQP1-expressing oocytes that were microinjected with carbonic anhydrase and impaled with pH-sensitive microelectrodes. Further work from the same group (Cooper & Boron, 1998) showed inhibition of CO<sub>2</sub> transport by *p*-chloromercuriphenylsulfonic acid (pCMBS) in oocytes expressing wild-type AQP1 but lesser inhibition in oocytes expressing an AQP1 mutant lacking the cysteine known to be involved in water transport inhibition. The facilitated transport of CO<sub>2</sub> by a membrane protein was a surprising observation given the very high CO<sub>2</sub> permeability of biological membranes and consequent unstirred layer effects that are predicted to preclude an increase in apparent membrane CO<sub>2</sub> permeability even if intrinsic membrane CO<sub>2</sub> permeability could increase. Nevertheless, the potential consequences of AQP1-mediated CO<sub>2</sub> permeability in mammalian physiology include AQP1-dependent CO<sub>2</sub> exchange in erythrocytes and lung, and possibly AQP1-dependent HCO<sub>3</sub><sup>-</sup> absorption by kidney

proximal tubule. AQP1 is strongly expressed in cell plasma membranes in erythrocytes, alveolar capillary endothelia and kidney proximal tubule epithelia, sites where it has been shown in knockout mice to constitute the major pathway for osmotically driven water transport (Ma *et al.* 1998; Schnermann *et al.* 1998; Bai *et al.* 1999; Chou *et al.* 1999).

We recently investigated the possibility of AQP1-mediated CO<sub>2</sub> transport by comparison of CO<sub>2</sub> permeabilities in erythrocytes of wild-type *vs.* AQP1 null mice, and in liposomes *vs.* AQP1-reconstituted proteoliposomes (Yang *et al.* 2000). Apparent CO<sub>2</sub> permeability was not impaired in erythrocytes lacking AQP1 despite a 7-fold reduced water permeability, nor was apparent CO<sub>2</sub> permeability increased in proteoliposomes despite a > 100-fold increased water permeability. A previous report of HgCl<sub>2</sub> inhibition of apparent CO<sub>2</sub> permeability in AQP1-containing proteoliposomes (Prasad *et al.* 1998) was confirmed, but the reduced CO<sub>2</sub> permeability was attributed to HgCl<sub>2</sub> inhibition of carbonic anhydrase (added to the liposome lumen) rather than to inhibition of AQP1. We also tested whether AQP1 deletion in mice affected the physiological exchange of CO<sub>2</sub> across the air-space–blood interface in lung. AQP1

deletion in mice did not affect the partial pressure of CO<sub>2</sub> in blood, nor the kinetics of CO<sub>2</sub> blow-off in anaesthetized, ventilated mice subject to an acute reduction in inspired CO<sub>2</sub> content from 5% to 0% (Yang *et al.* 2000). In those studies the mice were not stressed, so that CO<sub>2</sub> transport across the air-space–capillary barrier may have been limited by flow rather than diffusion and thus relatively insensitive to changes in the intrinsic CO<sub>2</sub> permeability of alveolar capillaries. We did not measure CO<sub>2</sub> or HCO<sub>3</sub><sup>-</sup> transport in perfused kidney proximal tubules from AQP1-null mice because unstirred layers would preclude meaningful measurement of CO<sub>2</sub> transport, and compensatory changes in transporter expression would preclude meaningful comparison of HCO<sub>3</sub><sup>-</sup> transport in wild-type *vs.* AQP1-null mice.

This paper is part of a special issue of *The Journal of Physiology* containing reviews and commentaries written in conjunction with a *Journal of Physiology*-sponsored symposium entitled 'Water Transport Controversies' that was held at the 2001 IUPS meeting in Christchurch, New Zealand. In addition to providing a commentary on the work of Professor Walter Boron and colleagues published in this issue (see Discussion), we report new data on CO<sub>2</sub> permeability in lung and kidney of wild-type *vs.* AQP1 null mice. Diffusion-limited CO<sub>2</sub> permeability was measured in isolated, rapidly perfused lungs utilizing a pleural surface fluorescence method in which changes in air-space fluid pH were followed in response to addition of HCO<sub>3</sub><sup>-</sup>/CO<sub>2</sub> to the pulmonary artery perfusate. CO<sub>2</sub> permeability of the proximal tubule cell luminal membrane was measured by a stopped-flow fluorescence method in isolated membrane vesicles. The new results extend our previous observations, and provide further evidence against physiologically important transport of CO<sub>2</sub> by AQP1.

## METHODS

### Transgenic mice

Transgenic knockout mice deficient in AQP1 or AQP5 in a CD1 genetic background were generated by targeted gene disruption (Ma *et al.* 1998, 1999). AQP1–AQP5 double knockout mice were generated by serial breeding of the single knockout mice (Ma *et al.* 2000). All animal procedures were approved by the University of California, San Francisco Committee on Animal Research.

### Isolated lung perfusion

Mice were killed with intraperitoneal pentobarbital (150 mg kg<sup>-1</sup>). The trachea was cannulated with polyethylene PE-90 tubing, and the pulmonary artery with PE-20 tubing. The left atrium was transected to permit fluid exit. The pulmonary artery was gravity perfused at constant pressure (25–30 cmH<sub>2</sub>O) at room temperature. More than 90% of lung perfusions were successful. The time between death and perfusion was generally < 7 min. The air-space was filled with 0.5 ml of a buffered isosmolar saline solution containing fluorescent indicators (see below).

### Pleural surface fluorescence measurements

Air-space fluid fluorescence was measured by a pleural surface fluorescence method (Carter *et al.* 1996). The heart and lungs

were positioned in a perfusion chamber for observation by epifluorescence microscopy. 2',7'-Bis(carboxyethyl)-5(6)-carboxyfluorescein (BCECF)–dextran (0.2 mg ml<sup>-1</sup>) was added to the air-space fluid as pH indicator or fluorescein isothiocyanate (FITC)–dextran (70 kDa, 0.5 mg ml<sup>-1</sup>) as a volume marker. The fluorescence from a 3–5 mm diameter spot on the lung pleural surface was monitored continuously with an inverted epifluorescence microscope using a ×10 air objective and filter set consisting of 490 ± 10 nm excitation filter, 510 nm dichroic mirror, and > 515 nm cut-on filter. Signals were detected by a photomultiplier, amplified, digitized and recorded at a rate of 1 Hz. Rates of airway fluid pH change were determined from the time course of BCECF–dextran fluorescence in response to CO<sub>2</sub>/HCO<sub>3</sub><sup>-</sup> gradients using an *in vitro* fluorescence *vs.* pH calibration. Osmotic water permeability (*P*<sub>f</sub>) was computed from the time course of FITC–dextran fluorescence in response to osmotic gradients as described previously (Carter *et al.* 1996).

### Measurement of air-space–capillary CO<sub>2</sub> and osmotic water permeabilities

CO<sub>2</sub> transport between the air-space and capillary compartments was determined from the time course of pleural surface fluorescence in response to exchange of CO<sub>2</sub>/HCO<sub>3</sub><sup>-</sup>-free and CO<sub>2</sub>/HCO<sub>3</sub><sup>-</sup>-containing perfusates. The air-space fluid contained 133 mM NaCl, 3 mM KCl, 0.68 mM CaCl<sub>2</sub>, 0.49 mM MgCl<sub>2</sub>, 1.5–2.5 mM sodium phosphate, and 1% bovine serum albumin (pH 7.4, 300 mosmol kg<sup>-1</sup>). The air-space instillate also contained 0.5–2.5 mg ml<sup>-1</sup> carbonic anhydrase (CA) to promote rapid CO<sub>2</sub>/HCO<sub>3</sub><sup>-</sup> equilibration. The CO<sub>2</sub>/HCO<sub>3</sub><sup>-</sup>-containing perfusate contained 25 mM NaHCO<sub>3</sub> instead of NaCl and was bubbled with 5% CO<sub>2</sub>. Osmotically driven water transport between the air-space and capillary compartment was measured as described previously (Bai *et al.* 1999; Song *et al.* 2000). The air-space fluid contained Hepes-buffered Ringer solution: 137 mM NaCl, 2.7 mM KCl, 1.25 mM MgSO<sub>4</sub>, 1.8 mM CaCl<sub>2</sub>, 5.5 mM glucose, 12 mM Hepes, 1% bovine serum albumin; pH 7.4, 300 mosmol kg<sup>-1</sup>. The perfusate was switched between osmolalities of 300 and 500 mosmol kg<sup>-1</sup> (sucrose added).

### Isolation and water permeability of proximal tubule apical membrane vesicles from mouse kidney

Sealed apical membrane vesicles from kidney proximal tubule were isolated by a magnesium aggregation procedure (Booth & Kenny, 1974; Ma *et al.* 1998). Osmotic water permeability in apical membrane vesicles was measured by stopped-flow light scattering as described previously (Ma *et al.* 1998).

### CO<sub>2</sub> permeability in apical membrane vesicles

Stopped-flow measurements were carried out on a Hi-Tech Sf-51 stopped-flow apparatus with dead time ~1.2 ms. Vesicles were labelled with the acetoxymethyl ester of BCECF (BCECF AM, Molecular Probes) by incubation with 20 μM BCECF AM in PBS at 22°C for 15 min. External dye was removed by four washes (12 000 g, 5 min). BCECF-labelled apical membrane vesicles were suspended at 5 mg protein ml<sup>-1</sup> in 110 mM NaCl, 5 mM KCl, 25 mM Hepes (bubbled for 30 min in N<sub>2</sub>) and mixed in the stopped-flow apparatus with an equal volume of 60 mM NaCl, 5 mM KCl, 50 mM NaHCO<sub>3</sub>, 25 mM Hepes titrated to give specified pH after mixing with an equal volume of the vesicle suspension. Solutions were incubated at least 2 h in a sealed flask to insure CO<sub>2</sub>/HCO<sub>3</sub><sup>-</sup> equilibration, and solution pH was checked before stopped-flow measurements. BCECF fluorescence was excited using a 485 ± 10 nm interference filter and detected using a > 515 nm cut-on filter. In some experiments, acetazolamide (0.1 mM) was added to the vesicle suspension. The apparent CO<sub>2</sub>

permeability coefficient ( $P_{\text{CO}_2}$ , cm s<sup>-1</sup>) was estimated as described previously (Yang *et al.* 2000) from an exponential time constant ( $\tau$ ) fitted to the fluorescence time course:

$$P_{\text{CO}_2} = (1/\tau)[(S/V)/10^{(\text{pH}_f - \text{pK}_a)}]^{-1},$$

where  $S/V$  is vesicle surface-to-volume ratio ( $2.5 \times 10^5 \text{ cm}^{-1}$ ),  $\text{pK}_a$  is 6.1, and  $\text{pH}_f$  is final intravesicular pH determined from the drop in BCECF fluorescence.

## RESULTS

### CO<sub>2</sub> permeability of the lung alveolar–capillary barrier

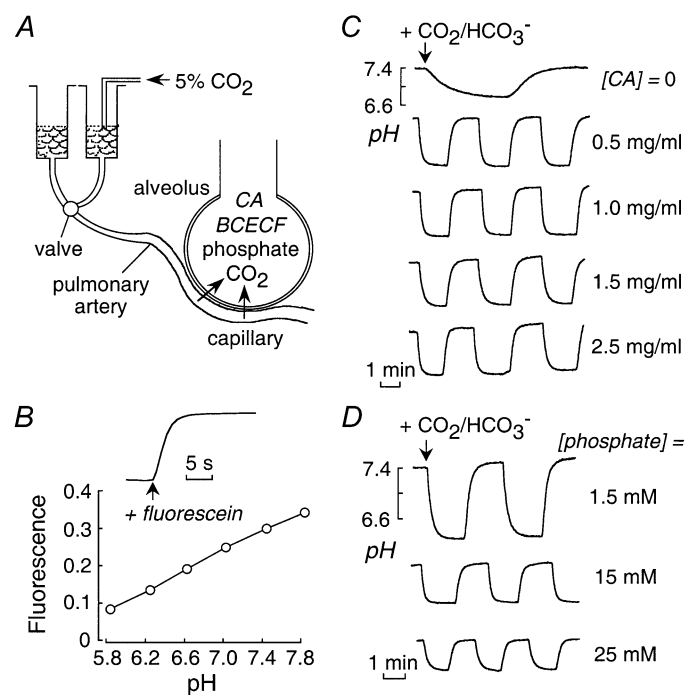
Figure 1A shows a schematic of the pleural surface method used to measure lung CO<sub>2</sub> permeability. The air-space was filled with CO<sub>2</sub>/HCO<sub>3</sub><sup>-</sup>-free fluid containing carbonic anhydrase to ensure rapid HCO<sub>3</sub><sup>-</sup>/CO<sub>2</sub>/pH equilibration, and BCECF–dextran to give a pH-dependent fluorescence signal that was detected at the lung surface. Rapid exchange of the pulmonary artery perfusate from a CO<sub>2</sub>/HCO<sub>3</sub><sup>-</sup>-free to a CO<sub>2</sub>/HCO<sub>3</sub><sup>-</sup>-containing solution resulted in CO<sub>2</sub> influx, producing a drop in pH and a decrease in BCECF fluorescence. The pH increased reversibly after return to a CO<sub>2</sub>/HCO<sub>3</sub><sup>-</sup>-free solution. Figure 1B (inset) shows the perfusate exchange time in these experiments as determined from the kinetics of pleural surface fluorescence following the exchange of a non-fluorescent to fluorescent perfusate. The half-equilibration time ( $t_{1/2}$ ) was 1.3 s. Figure 1B shows that BCECF–dextran fluorescence is sensitive to pH in the range appropriate for the experiments here. By stopped-flow analysis, BCECF–dextran fluorescence responded in < 1 ms to pH changes in the pH range 6–8 (data not shown). These experiments demonstrate the suitability of the pleural surface fluorescence method to detect rapid air-space–capillary CO<sub>2</sub> exchange.

#### Figure 1. Air space–capillary CO<sub>2</sub> transport in mouse lung measured by a pleural surface fluorescence method

A, schematic showing an isolated perfused mouse lung. The air-space fluid contains carbonic anhydrase and the fluorescent pH indicator BCECF–dextran. The pulmonary artery perfusate was exchanged between isosmolar CO<sub>2</sub>/HCO<sub>3</sub><sup>-</sup>-free and CO<sub>2</sub>/HCO<sub>3</sub><sup>-</sup>-containing solutions. CO<sub>2</sub>/HCO<sub>3</sub><sup>-</sup> addition results in acidification of air-space fluid and a decrease in pleural surface BCECF–dextran fluorescence. B, relationship between BCECF–dextran fluorescence and pH. Inset, perfusate exchange rate. Time course of pleural surface fluorescence in response to exchange between non-fluorescent and fluorescent (containing FITC–dextran) perfusates. Perfusate flow rate was 3–5 ml min<sup>-1</sup>, as in subsequent CO<sub>2</sub> transport measurements. C, time course of air-space fluid pH (computed from pleural surface fluorescence) in response to exchange between CO<sub>2</sub>/HCO<sub>3</sub><sup>-</sup>-free and CO<sub>2</sub>/HCO<sub>3</sub><sup>-</sup>-containing perfusates. Air-space fluid contained carbonic anhydrase (CA) at indicated concentrations. D, same as in C (with 1 mg ml<sup>-1</sup> CA) in which the air-space instillate contained indicated amounts of phosphate buffer.

Figure 1C shows representative time courses of air-space fluid pH in response to exchange between CO<sub>2</sub>/HCO<sub>3</sub><sup>-</sup>-free and CO<sub>2</sub>/HCO<sub>3</sub><sup>-</sup>-containing pulmonary artery perfusates. The pH equilibration was slow in the absence of carbonic anhydrase in the air-space fluid (top curve). The pH equilibration was rapid ( $t_{1/2} \approx 5.6$  s) and reversible in the presence of carbonic anhydrase. The equilibration time was not sensitive to carbonic anhydrase concentration in range 0.5–2.5 mg ml<sup>-1</sup>, as predicted from the millisecond kinetics of CO<sub>2</sub>/HCO<sub>3</sub><sup>-</sup> equilibration at these concentrations reported in previous stopped-flow measurements (Yang *et al.* 2000). The magnitude of the pH drop was sensitive to air-space fluid buffer capacity, increasing from 0.47 to 1.3 pH units for air-space solutions containing 25 and 1.5 mM phosphate, respectively (Fig. 1D). The non-linear dependence of the drop in pH on instillate buffer capacity indicates that the alveolar lumen contains endogenous buffers such as cell surface proteins.

Measurements of air-space–capillary CO<sub>2</sub> exchange were done in wild-type mice, and mice lacking AQP1 and AQP5, individually and together. Representative fluorescence time course data in Fig. 2A (left) show no apparent effect of aquaporin deletion. Measurement of air-space–capillary osmotically induced water permeability showed marked reduction in water permeability in the aquaporin-null mice (Fig. 2A, right). Water permeability was 10-fold reduced by deletion of AQP1 or AQP5 separately, and was further reduced ~3 fold by their deletion together. Figure 2B (top) shows the direct comparison on an expanded time scale of changes of air-space fluid pH following CO<sub>2</sub>/HCO<sub>3</sub><sup>-</sup> addition and removal. Figure 2B (bottom) summarizes the rates of CO<sub>2</sub> influx and efflux for lungs from a series of mice. There was no significant effect of aquaporin deletion on air-space–capillary CO<sub>2</sub> transport.



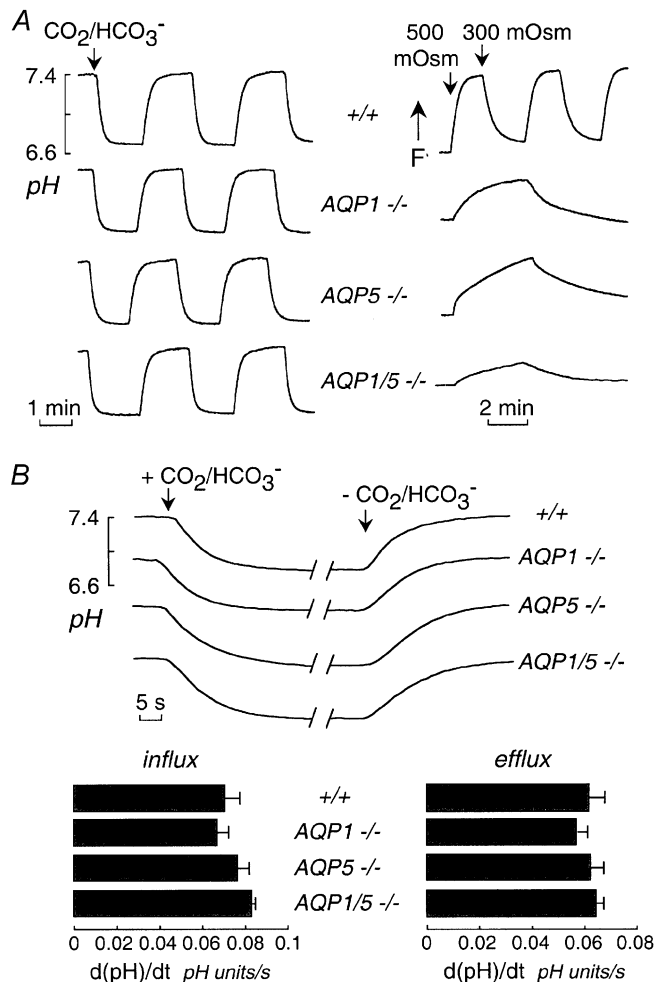


**Figure 2. Influence of aquaporin deletion on air-space-capillary  $\text{CO}_2$  and osmotic water permeabilities**

A, left,  $\text{CO}_2$  permeability in lungs from mice of indicated genotype. Time course of air-space fluid pH in response to exchange between  $\text{CO}_2/\text{HCO}_3^-$ -free and  $\text{CO}_2/\text{HCO}_3^-$ -containing perfusates measured as in Fig. 1C. The air-space instillate contained  $1 \text{ mg ml}^{-1}$  CA and the perfusate contained 0 or  $25 \text{ mM HCO}_3^-$ . Right, osmotic water permeability. Time course of air-space fluid osmolality (measured by FITC-dextran fluorescence) in response to exchange between perfusates of osmolality 300 and  $500 \text{ mosmol kg}^{-1}$ . B, top, representative time course data as in A (left) shown on an expanded time scale. Bottom, summary of rates of  $\text{CO}_2$  transport into and out of the air-space fluid. Data are shown as mean and S.E.M. for  $n = 3-5$  lungs per group. Differences not significant.

### $\text{CO}_2$ permeability of proximal tubule vesicles

Figure 3A shows osmotic water permeability in suspended proximal tubule vesicles measured by stopped-flow light scattering. Osmotic water permeability coefficients ( $P_f$ ) were  $0.039 \pm 0.002 \text{ cm s}^{-1}$  (wild-type) and  $0.0020 \pm 0.0002 \text{ cm s}^{-1}$  (AQP1 null), indicating that AQP1 provides the major route for water transport in these membranes. The low  $P_f$  after AQP1 deletion suggests water movement across the lipid bilayer.

$\text{CO}_2$  transport was measured from the kinetics of intravesicular acidification following rapid mixture of vesicles suspended in a  $\text{CO}_2/\text{HCO}_3^-$ -free buffer with an isosmolar buffer containing  $\text{CO}_2/\text{HCO}_3^-$ . Intravesicular  $\text{CO}_2/\text{HCO}_3^-/\text{pH}$  equilibration is facilitated by the endogenous membrane-associated carbonic anhydrase (type IV) present on proximal tubule cell membranes (Maren *et al.* 1993; Brion *et al.* 1997). The vesicles were loaded with the fluorescent pH indicator BCECF by incubation with BCECF AM followed

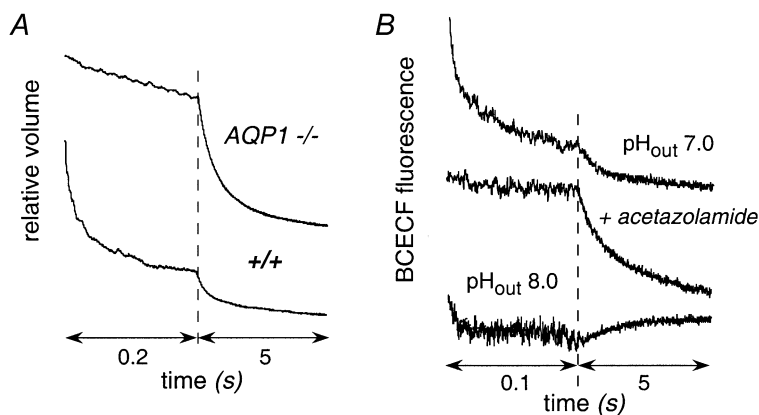


**Figure 3. Osmotic water permeability and  $\text{CO}_2$  permeability in apical membrane vesicles from mouse kidney proximal tubule**

A, vesicles were subjected to a  $250 \text{ mM}$  inwardly directed sucrose gradient at  $10^\circ\text{C}$ . Data are plotted using two contiguous times scales to show the complete osmotic equilibration. B, vesicles were loaded with the fluorescent pH indicator BCECF and suspended in an isosmolar buffer at pH 7.4 (not containing  $\text{CO}_2/\text{HCO}_3^-$ , see Methods). The suspension was mixed in a stopped-flow apparatus with appropriate buffers to give  $25 \text{ mM CO}_2/\text{HCO}_3^-$  at pH 7.0 or 8.0. Where indicated, vesicles were incubated with acetazolamide prior to the assay. Curves have been displaced arbitrarily in the  $y$ -direction for clarity.



by extensive washing. The intravesicular de-esterification of BCECF AM in these vesicles is thought to arise in part from carbonic anhydrase activity, so that vesicles containing higher amounts of carbonic anhydrase are preferentially labelled. Figure 3B shows the time course of intravesicular BCECF fluorescence following exposure of proximal tubule vesicles (from wild-type mice) to a CO<sub>2</sub>-equilibrated solution containing 25 mM HCO<sub>3</sub><sup>-</sup> at indicated pH<sub>out</sub>. There was a biphasic time course of decreasing fluorescence, with 75–80% of the signal dropping very rapidly ( $t_{1/2} \approx 10$  ms) and the remaining signal dropping over ~300 ms. The rapid phase of decreasing fluorescence probably corresponds to CO<sub>2</sub> transport in a population of proximal tubule apical membrane vesicles containing relatively large amounts of carbonic anhydrase; the slower signal component may correspond to contaminating vesicles or vesicles from regions of the proximal tubule containing less carbonic anhydrase. This interpretation is supported by the slowed acidification after incubation of vesicles with the carbonic anhydrase inhibitor acetazolamide (Fig. 3B, second curve). As expected, the magnitude of the prompt intracellular acidification was decreased with increasing extracellular pH because of the decrease in CO<sub>2</sub>/HCO<sub>3</sub><sup>-</sup> ratio (Fig. 3B, third curve).

CO<sub>2</sub> permeability was compared in proximal tubule vesicles isolated from kidneys of three wild-type and three AQP1-null mice. Representative stopped-flow data are given in Fig. 4A, showing similar kinetics of acidification in vesicles from wild-type and AQP1-null mice. Figure 4B summarizes apparent CO<sub>2</sub> permeability coefficients ( $P_{\text{CO}_2}$ ) computed from acidification rates, final intravesicular pH, and vesicle geometry (see Methods).  $P_{\text{CO}_2}$  was not significantly affected by AQP1 deletion:  $0.0034 \pm 0.0005$  cm s<sup>-1</sup> (wild-type) and  $0.0035 \pm 0.0006$  cm s<sup>-1</sup> (AQP1 null).

## DISCUSSION

The experiments here address whether transport of CO<sub>2</sub> by AQP1 is physiologically important in lung and kidney. Measurements in the isolated perfused lung under diffusion-limited conditions extend previous data in living ventilated mice showing no effect of AQP1 deletion on CO<sub>2</sub> transport across the air-space–capillary barrier. The measurements in kidney proximal tubule vesicles indicate that CO<sub>2</sub> transport across the proximal tubule apical membrane is rapid and not affected by AQP1 deletion. Additional comments follow, after which general issues with regard to aquaporin-mediated CO<sub>2</sub> transport are discussed.

The exchange of CO<sub>2</sub> between the air-space and erythrocytes in alveolar capillaries involves CO<sub>2</sub> movement across the alveolar epithelium and endothelium, and the erythrocyte membrane, as well as CO<sub>2</sub> diffusion through the lung interstitium and serum. CO<sub>2</sub> transport across the erythrocyte membrane is not rate limiting in air-space–erythrocyte

CO<sub>2</sub> exchange since CO<sub>2</sub> equilibration in erythrocytes occurs within a few milliseconds (Yang *et al.* 2000) and is facilitated by anion exchange of HCO<sub>3</sub><sup>-</sup> catalysed by carbonic anhydrase. The question addressed here is whether aquaporin-dependent CO<sub>2</sub> transport across the alveolar barriers facilitates air-space–capillary CO<sub>2</sub> equilibration. CO<sub>2</sub> transport into and out of the air-space was measured by a kinetic approach, from the time course of air-space fluid pH in response to changes in the CO<sub>2</sub>/HCO<sub>3</sub><sup>-</sup> content of fluid perfused rapidly through the pulmonary artery. Changes in air-space CO<sub>2</sub> content were followed from the fluorescence of a pH indicator in the air-space fluid using carbonic anhydrase to ensure rapid HCO<sub>3</sub><sup>-</sup>/CO<sub>2</sub> and thus pH equilibration. Stopped-flow measurements showed previously that HCO<sub>3</sub><sup>-</sup>/CO<sub>2</sub>/pH equilibration occurs in < 1 ms, a time much faster than that of alveolar–capillary CO<sub>2</sub> exchange measured here. The rapid pulmonary artery perfusion and the measurement of pH in a small volume of air-space fluid by the pleural surface fluorescence method minimized effects of uneven capillary perfusion.

We found that CO<sub>2</sub> exchange across the lung alveolar epithelial and endothelial barriers was rapid and not affected by deletion of AQP1 and/or AQP5, whereas osmotically induced water permeability was reduced by up to 30-fold. The time for pH equilibration was much slower than the time for perfusate exchange as measured by addition of a fluorescent marker to one of the perfusates. Aquaporin-mediated CO<sub>2</sub> transport thus does not contribute to CO<sub>2</sub> equilibration across the air-space–capillary barrier.

CO<sub>2</sub> transport across the AQP1-containing apical membrane of kidney proximal tubule was measured from the rate of acidification in apical membrane vesicles following rapid exposure to CO<sub>2</sub>/HCO<sub>3</sub><sup>-</sup> in a stopped-flow apparatus. Measurement of CO<sub>2</sub> transport in small suspended vesicles is advantageous to measurements in intact proximal tubule because more rapid mixing is possible, and because the small size and single barrier structure of vesicles

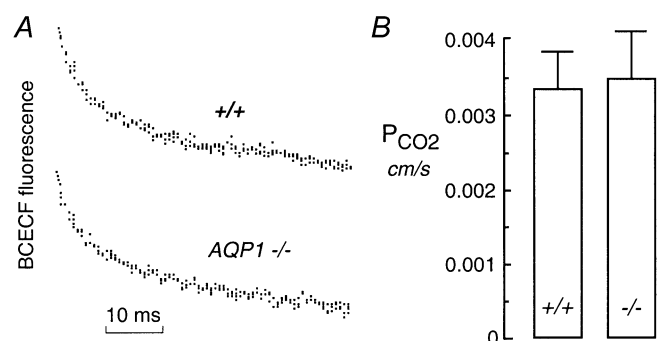


**Figure 4. Influence of AQP1 deletion on CO<sub>2</sub> permeability in apical membrane vesicles from proximal tubule**

A, vesicles were subjected to a 25 mM CO<sub>2</sub>/HCO<sub>3</sub><sup>-</sup> gradient at a final outside pH of 7.0 as in Fig. 3B. B, averaged  $P_{\text{CO}_2}$  computed from experiments as in A. Data are means and S.E.M.

**Table 1. CO<sub>2</sub> permeabilities ( $P_{\text{CO}_2}$ ) of lipid bilayers and biological membranes**

System	Measurement method	$P_{\text{CO}_2}$ (cm s <sup>-1</sup> )	Reference
Planar bilayer	pH measurements	0.35	Gutknecht <i>et al.</i> 1977
Erythrocyte	Mass spectrometry	~1	Forster <i>et al.</i> 1998
	Luminal pH kinetics	0.01	Yang <i>et al.</i> 2000
	Luminal pH kinetics	0.001	Yang <i>et al.</i> 2000
Liposome	Luminal pH kinetics	0.001	Yang <i>et al.</i> 2000
Proximal tubule vesicle	Luminal pH kinetics	0.0035	This paper
Corneal cell cultures	Cytoplasmic pH (BCECF)	0.0036	Sun <i>et al.</i> 2001
<i>Xenopus</i> oocyte	pH microelectodes	0.006	Nakhoul <i>et al.</i> 1998

minimizes unstirred layer effects. We found rapid CO<sub>2</sub> transport across the proximal tubule apical membrane that was not affected by AQP1 deletion. It is thus unlikely that CO<sub>2</sub> transport by AQP1 could augment proximal tubule HCO<sub>3</sub><sup>-</sup> absorption. Indeed, the data of Vallon *et al.* (2000), in which end-proximal tubule micropuncture samples were analysed for tubular fluid osmolarity and chloride concentration, provided evidence against significant accumulation of HCO<sub>3</sub><sup>-</sup> at the end proximal tubule of AQP1-null mice. AQP1 deficiency in mice generates marked luminal hypotonicity in proximal tubules, indicating that near-isosmolar fluid absorption requires functional AQP1. However, ion/HCO<sub>3</sub><sup>-</sup> transport data in AQP1-null mice should be viewed cautiously because of compensatory changes in proximal tubule transporter expression. When available, potent non-toxic AQP1 inhibitors will be useful in defining the role of AQP1 in complex systems involving osmotic and electrochemical gradients produced by multiple interacting transporting systems.

A concern in the measurement of CO<sub>2</sub> permeability across highly CO<sub>2</sub>-permeable biological membranes is unstirred layer effects. Diffusion of CO<sub>2</sub> in unstirred aqueous solutions adjacent to membranes is generally substantially slower than CO<sub>2</sub> transport across the membrane itself. However, we note that unstirred layer effects in experimental models of CO<sub>2</sub> transport are relevant *in vivo*, so that augmentation of CO<sub>2</sub> transport by an aquaporin or other protein would be possible only when intrinsic membrane CO<sub>2</sub> permeability is exceptionally low, or by some unusual mechanism involving spatially organized CO<sub>2</sub> generation and channelling.

Unstirred layer effects are predicted to be greatest for large and complex cellular systems and when CO<sub>2</sub> diffusion is slowed by high cytoplasmic viscosity as expected in *Xenopus* oocytes. With respect to CO<sub>2</sub> transport, intrinsic membrane permeabilities have been estimated by extrapolation of CO<sub>2</sub> transport rates at high pH in the presence of carbonic anhydrase where CO<sub>2</sub> is rapidly created/dissipated near membranes by high concentrations of HCO<sub>3</sub><sup>-</sup> (Suchdeo & Schultz, 1973; Geers & Gros, 2000). As summarized in

Table 1, the true CO<sub>2</sub> permeability ( $P_{\text{CO}_2}$ ) across planar lipid bilayer is very high (~0.35 cm s<sup>-1</sup>, Gutknecht *et al.* 1977). A clever approach to estimate true CO<sub>2</sub> permeability in erythrocytes by establishing a quasi-steady-state CO<sub>2</sub> profile (Forster *et al.* 1998) also indicated a very high membrane  $P_{\text{CO}_2}$  of ~1 cm s<sup>-1</sup>. More conventional CO<sub>2</sub> mixing approaches, which are relevant *in vivo*, give substantially lower  $P_{\text{CO}_2}$  values of < 0.01 cm s<sup>-1</sup> as summarized in Table 1 for erythrocytes, liposomes, kidney vesicles and *Xenopus* oocytes. It is thus likely that CO<sub>2</sub> transport in each of these cases is unstirred-layer limited and so not sensitive to intrinsic membrane CO<sub>2</sub> permeability. Thus, as discussed previously (Yang *et al.* 2000), we can only report an upper limit to the quantity of CO<sub>2</sub> transported by individual AQP1 monomers. With regard to mammalian physiology, direct evidence in erythrocytes, lung and kidney argues strongly against physiologically important transport of CO<sub>2</sub> by AQP1.

In conclusion, the transport of small gases by aquaporins is an interesting hypothesis, though from the experiments reported here, and based on general principles, physiologically significant transport of CO<sub>2</sub> by AQP1 is unlikely. We showed previously that NH<sub>3</sub> transport in erythrocytes, which is relatively slow and thus not unstirred-layer limited, is not affected by AQP1 deletion (Yang *et al.* 2000). Aquaporin-mediated transport of other small gases (O<sub>2</sub>, CO, NO) may warrant investigation; however, the high intrinsic membrane permeabilities for these gases makes aquaporin-facilitated transport unlikely. Finally, transport measurements of CO<sub>2</sub>, NH<sub>3</sub> and other small gases by the aquaglyceroporins (AQP3, AQP7 and AQP9) may be interesting. These proteins are able to transport glycerol and some small solutes along with water, and so may contain a relatively wide, non-selective pore.

## REFERENCES

- BAI, C., FUKUDA, N., SONG, Y., MA, T., MATTHAY, M. A. & VERKMAN, A. S. (1999). Lung fluid transport in aquaporin-1 and aquaporin-4 knockout mice. *Journal of Clinical Investigation* **103**, 555–561.
- BOOTH, A. G. & KENNY, A. J. (1974). A rapid method for the preparation of microvilli from rabbit kidney. *Biochemical Journal* **142**, 575–581.

- BRION, L. P., CAMMER, W., SATLIN, L. M., SUAREZ, C., ZAVILOWITZ, B. J. & SCHUSTER, V. L. (1997). Expression of carbonic anhydrase IV in carbonic anhydrase II-deficient mice. *American Journal of Physiology* **273**, F234–245.
- CARTER, E. P., MATTHAY, M. A., FARINAS, J. & VERKMAN, A. S. (1996). Transalveolar osmotic and diffusional water permeability in intact mouse lung measured by a novel surface fluorescence method. *Journal of General Physiology* **108**, 133–142.
- CHOU, C. L., KNEPPER, M. A., HOEK, A. N., BROWN, D., YANG, B., MA, T. & VERKMAN, A. S. (1999). Reduced water permeability and altered ultrastructure in thin descending limb of Henle in aquaporin-1 null mice. *Journal of Clinical Investigation* **103**, 491–496.
- COOPER, G. J. & BORON, W. F. (1998). Effect of PCMBs on CO<sub>2</sub> permeability of *Xenopus* oocytes expressing aquaporin 1 or its C189S mutant. *American Journal of Physiology* **275**, C1481–1486.
- FORSTER, R. E., GROS, G., LIN, L., ONO, Y. & WUNDER, M. (1998). The effect of 4,4'-diisothiocyanato-stilbene-2,2'-disulfonate on CO<sub>2</sub> permeability of the red blood cell membrane. *Proceedings of the National Academy of Sciences of the USA* **95**, 15815–15820.
- GEERS, C. & GROS, G. (2000). Carbon dioxide transport and carbonic anhydrase in blood and muscle. *Physiological Reviews* **80**, 681–715.
- GUTKNECHT, J., BISSON, M. A. & TOSTESON, F. C. (1977). Diffusion of carbon dioxide through lipid bilayer membranes: effects of carbonic anhydrase, bicarbonate, and unstirred layers. *Journal of General Physiology* **69**, 779–794.
- MA, T., FUKUDA, N., SONG, Y., MATTHAY, M. A. & VERKMAN, A. S. (2000). Lung fluid transport in aquaporin-5 knockout mice. *Journal of Clinical Investigation* **105**, 93–100.
- MA, T., SONG, Y., GILLESPIE, A., CARLSON, E. J., EPSTEIN, C. J. & VERKMAN, A. S. (1999). Defective secretion of saliva in transgenic mice lacking aquaporin-5 water channels. *Journal of Biological Chemistry* **274**, 20071–20074.
- MA, T., YANG, B., GILLESPIE, A., CARLSON, E. J., EPSTEIN, C. J. & VERKMAN, A. S. (1998). Severely impaired urinary concentrating ability in transgenic mice lacking aquaporin-1 water channels. *Journal of Biological Chemistry* **273**, 4296–4299.
- MAREN, T. H., WYNNS, G. C. & WISTRAND, P. J. (1993). Chemical properties of carbonic anhydrase IV, the membrane-bound enzyme. *Molecular Pharmacology* **44**, 901–905.
- NAKHOUL, N. L., DAVIS, B. A., ROMERO, M. F. & BORON, W. F. (1998). Effect of expressing the water channel aquaporin-1 on the CO<sub>2</sub> permeability of *Xenopus* oocytes. *American Journal of Physiology* **274**, C543–548.
- PRASAD, G. V., COURY, L. A., FINN, F. & ZEIDEL, M. L. (1998). Reconstituted aquaporin 1 water channels transport CO<sub>2</sub> across membranes. *Journal of Biological Chemistry* **273**, 33123–33126.
- SCHNERMANN, J., CHOU, C. L., MA, T., TRAYNOR, T., KNEPPER, M. A. & VERKMAN, A. S. (1998). Defective proximal tubular fluid reabsorption in transgenic aquaporin-1 null mice. *Proceedings of the National Academy of Sciences of the USA* **95**, 9660–9664.
- SONG, Y., MA, T., MATTHAY, M. A. & VERKMAN, A. S. (2000). Role of aquaporin-4 in airspace-to-capillary water permeability in intact mouse lung measured by a novel gravimetric method. *Journal of General Physiology* **115**, 17–27.
- SUCHDEO, S. & SCHULTZ, J. S. (1973). Effect of carbonic anhydrase on the facilitated diffusion of CO<sub>2</sub> through bicarbonate solutions. *Advances in Experimental Medicine and Biology* **37**, 969–974.
- SUN, X. C., XIE, Q., STAMER, W. D. & BONANNO, J. A. (2001). Effect of AQP1 expression level on CO<sub>2</sub> permeability in bovine corneal endothelium. *Investigative Ophthalmology and Visual Science* **42**, 417–423.
- VALLON, V., VERKMAN, A. S. & SCHNERMANN, J. (2000). Luminal hypotonicity in proximal tubules of aquaporin-1-knockout mice. *American Journal of Physiology – Renal Physiology* **278**, F1030–1033.
- YANG, B., FUKUDA, N., VAN HOEK, A., MATTHAY, M. A., MA, T. & VERKMAN, A. S. (2000). Carbon dioxide permeability of aquaporin-1 measured in erythrocytes and lung of aquaporin-1 null mice and in reconstituted proteoliposomes. *Journal of Biological Chemistry* **275**, 2686–2692.

#### Acknowledgements

This work was supported by grants DK35124, HL59198, HL51856, HL60288 and DK43840 from the National Institutes of Health and a grant from the Cystic Fibrosis Foundation.